Proceedings of the 2003 IEEE International Frequency Control Symposium and PDA Exhibition
Jointly with the 17th European Frequency and Time Forum

Chemical Liquid-Phase Detection Using Guided SH-SAW: Theoretical Simulation and Experiments

Zhonghui Li, Yolanda Jones[1], Jeanne Hossenlopp[1], Richard Cernosek[2] and Fabien Josse

Microsensor Research Laboratory and Department of Electrical and Computer Engineering, [1]Department of Chemistry, Marquette University, P.O. Box 1881, Milwaukee, WI 53201-1881,
[2]Micro-Analytical Systems Dept., Sandia National Laboratories, P.O. Box 5800, MS 0892, Albuquerque, NM 87185-0892

Abstract **- Results are presented for direct chemical sensing in liquid environments using guided shear horizontal surface acoustic wave (SH-SAW) sensor platforms on 36° rotated Y-cut $LiTaO_3$. Two different sensor geometries are theoretically analyzed. Complex bulk and shear moduli are utilized to represent the viscoelastic properties of the polymers and estimate their influence on the velocity shift and attenuation change, hence on the sensor characteristics. Experimental results are presented and discussed for dual delay line devices with a reference line coated with PMMA and a sensing line coated with a chemically sensitive polymer, which acts as both a guiding layer and a sensing layer. Various chemically sensitive polymers are investigated, and the tested analytes include toluene, ethylbenzene and xylene. Analytes in the low concentration (1 ppm to 60 ppm) range in aqueous solutions are tested. Stability, sensitivity and partial selectivity are investigated by varying the coating thickness and curing temperature for the chemically sensitive layer. Partition coefficients for polymer-aqueous analyte pairs are used to explain the observed trend in sensitivity. Both mass loading and the coating viscoelasticity change influence the sensor response. A low ppb level detection limit is estimated from the present experiment measurement.**

Keywords**: guided SH-SAW, chemical sensor, liquid-phase detection**

I. INTRODUCTION

Acoustic wave sensors have been extensively and successfully investigated for the detection of various (bio-) chemical compounds in gaseous environments [1]. Following successful application in gas sensing, liquid sensors attracted considerable attention due to the need for real-time, rapid and direct detection in liquid environments where the device is in direct contact with the solution [1-5].

Different types of acoustic waves have being studied, including thickness shear mode (TSM), shear horizontal acoustic plate mode (SH-APM), shear horizontal surface acoustic wave (SH-SAW), and flexural plate wave (FPW), etc. Of all acoustic wave devices, guided SH-SAW devices appear most promising for (bio-) chemical sensing in liquid environments, with the possibility of tailoring the device sensitivity [2-6]. Guided SH-SAW sensor (also known as Love-wave sensor) consists of a SH-SAW device, with an overlayer having a lower shear wave velocity. The purpose of the overlayer is to trap the acoustic energy near the sensing surface, thus making the device more sensitive to surface perturbations. Moreover, a liquid sample can be applied on the device surface without significantly damping the wave. In the present work, SH-SAW devices on 36° rotated Y-cut X propagating $LiTaO_3$ are used. A dual delay line configuration is used to make all the secondary interaction controls, such as temperature control, basically unnecessary. A metallized delay path between input and output IDTs is used to eliminate acousto-electric interactions with the load. Most polymers can be used as the thin guiding layer because of their relatively low shear wave velocity and the ease of surface layer preparation. To decrease the acoustic loss, cross-linking or curing of the polymer coating is necessary. However, a degree of signal attenuation is still needed to suppress the triple transit echo (TTE), which may add to the sensor noise and non-reproducibility. In the present paper, theoretical modeling is presented using two multilayer sensor geometries followed with a number of experiments. The objective here is to identify the various material parameter effects in the sensor response for further sensor optimization.

II. THEORETICAL ANALYSIS

The theoretical 3-layer (substrate - polymer coating layer - liquid layer) and 4-layer (substrate - polymer coating layer1 -polymer coating layer2 - liquid layer) geometries of the sensing system used are shown in Fig.1. In the 3-layer geometry, the viscoelastic layer serves both as waveguiding layer and chemical sensitive layer while in the 4-layer geometry, layer 1 works as waveguiding layer, and layer 2 acts as chemical sensitive layer only. The liquid layer is assumed to be a Newtonian fluid because solutions of interest are very dilute aqueous solutions. The liquid layer and substrate are considered as semi-infinite layers while the polymer coating is considered as a finite layer.

A complex propagating factor β is assumed and is defined by the wavenumber k and attenuation α as

$$\beta = k - j\alpha = \frac{\omega}{V} - j\alpha \qquad \textbf{(1)}$$

Here V is the phase velocity of the SH-SAW, and ω is the angular excitation frequency. The variation of the complex propagation constant is derived as

$$\frac{\Delta\beta}{k} = -\frac{\Delta V}{V} - j\frac{\Delta\alpha}{k} \qquad \textbf{(2)}$$

where ΔV and Δα are the changes in V and α, respectively. All quantities have been normalized by the wavenumber *k*. Using perturbation theory and surface acoustic impedance techniques [7,8], the variation in the complex propagation constant can be expressed as [9,10]

$$\frac{\Delta\beta}{k} = -\frac{jV(v^* \cdot Z_A^{'} \cdot v + v \cdot Z_A^* \cdot v^*)}{4\omega P} \quad \textbf{(3)}$$

where Z_A and v are the surface acoustic impedance and particle velocity amplitudes, respectively; * is the complex conjugate; ' is the perturbed term; P is the SH-SAW acoustic power density (power per unit width). In deriving (3), only a mechanical perturbation is assumed, with the surface electrically shorted. It is also assumed that only the surface stress is perturbed, and the particle velocity amplitude does not vary. Using (2) and (3), the relative change in velocity and the normalized attenuation are expressed as

$$\frac{\Delta V}{V} = \mathrm{Re}[\frac{jV(v^* \cdot Z_A^{'} \cdot v + v \cdot Z_A^* \cdot v^*)}{4\omega P}] \quad \textbf{(4a)}$$

$$\frac{\Delta\alpha}{k} = \mathrm{Im}[\frac{jV(v^* \cdot Z_A^{'} \cdot v + v \cdot Z_A^* \cdot v^*)}{4\omega P}] \quad \textbf{(4b)}$$

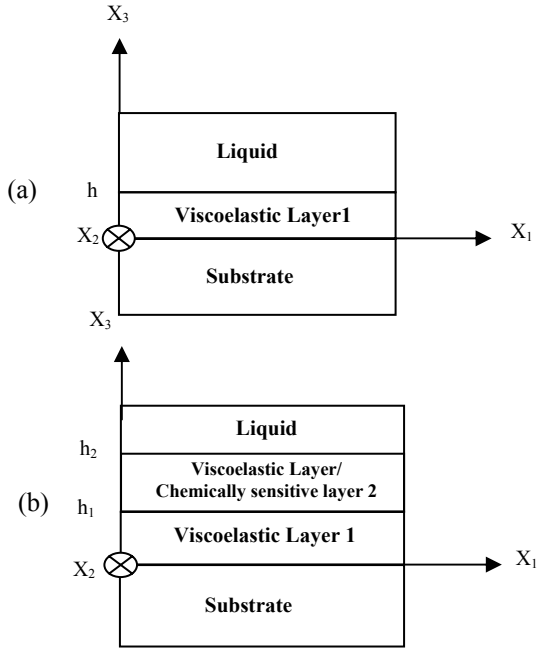

Fig. 1. Geometries representing the chemical sensor configurations. Also shown is the coordinate system used in the modeling. Only mechanical perturbation is assumed. (a) 3-layer; (b) 4-layer

Here the theoretical analysis will utilize the acoustic impedance at the surface before and after perturbation by the liquid sensing.

A. 3-layer structure modeling

1) The wave solution in the viscoelastic coating layer is written as[1]:

$$u_i^f(x_3) = A_i e^{j\beta_i x_3} + B_i e^{-j\beta_i x_3} \quad \textbf{(5a)}$$

where the parameters A_i and B_i are amplitude constants and

$$\beta_i = \omega(\frac{\rho_f - E_f^{(i)}/V^2}{M_f^{(i)}})^{1/2}$$

β_i is the complex propagation factor for displacement u_i (i=1,2,3) propagating across film; $M_f^{(i)}$ is the generalized modulus for the film layer; $E_f^{(i)}$ is the Young's modulus for the polymer coating layer generated by *i*th displacement component; and ρ_f is the mass density of the film. The cross-film gradient gives rise to the stress, T_{i3}, (force per area in the ith direction in planes parallel to the X_3-direction)

$$T_{i3}^f = M_f^{(i)} \frac{\partial u_i^f}{\partial x_3} \quad \textbf{(5b)}$$

2) The wave equation in the liquid layer can be expressed as

$$u_i^l(x_3) = C_i e^{-\beta_c(x_3 - h)} \quad \textbf{(6a)}$$

where

$$\beta_c = \frac{1+j}{\delta_l} \qquad \delta_l = \frac{2\eta_l}{\omega\rho_l}$$

The stress is given by

$$T_{i3}^l = M_l^{(i)} \frac{\partial u_i^l}{\partial x_3} \quad \textbf{(6b)}$$

Here $M_l^{(i)}$ is the generalized modulus for the liquid layer; $E_l^{(i)}$ is the Young's modulus for the liquid layer generated by *i*th displacement component; δ_l is the liquid decay length; η_l is the viscosity of the liquid; ρ_l is the mass density of the liquid and β_c is the complex shear wave propagating constant across liquid.

3) The boundary conditions are the continuity of the particle displacement and stress at various interfaces and are given by,

$$u_i^f(0) = u_{i0} \qquad u_i^f(h) = u_i^l(h) \qquad T_{i3}^f(h) = T_{i3}^l(h) \quad \textbf{(7)}$$

with u_{i0} the particle displacement of the substrate at the coating/substrate interface. Applying (7) at the viscoelastic layer/substrate interface and the viscoelastic layer/liquid interface, the three unknowns A_i, B_i and C_i can be found in terms of the properties of the piezoelectric material, polymer and liquid.

4) The perturbed surface acoustic impedance, $Z_A^{'}$, obtained from the wave solution and the stress, is given by

$$Z_A^{'} = \begin{bmatrix} \frac{\beta_1 M_f^1}{\omega} F_1 & 0 & 0 \\ 0 & \frac{\beta_2 M_f^2}{\omega} F_2 & 0 \\ 0 & 0 & \frac{\beta_3 M_f^3}{\omega} F_3 \end{bmatrix} \quad \textbf{(8)}$$

where

$$F_i = \frac{[(j\beta_i M_f^{(i)} + \beta_c M_l^{(i)})e^{j\beta_i h} - (j\beta_i M_f^{(i)} - \beta_c M_l^{(i)})e^{-j\beta_i h}]}{[(j\beta_i M_f^{(i)} + \beta_c M_l^{(i)})e^{j\beta_i h} + (j\beta_i M_f^{(i)} - \beta_c M_l^{(i)})e^{-j\beta_i h}]}$$

[1] Superscript or subscript f means film; l means liquid

From (8), it is seen that the sensor performance described by (4), is a function of polymer material parameters (mass density, viscoelasticity, film thickness) and the solution parameters. β_i, $M_f^{(i)}$ are polymer-dependent parameters and β_c, $M_l^{(i)}$ are liquid-dependent parameters. Obviously, one can analyze F_i to characterize the weight of each parameter.

B. 4-layer structure modeling

Similarly, the acoustic impedance, $Z_A^{'}$, for this structure is given by:

$$Z_A^{'} = \begin{bmatrix} \frac{\beta_{21} M_{f2}^{(1)}}{\omega} F_1 & 0 & 0 \\ 0 & \frac{\beta_{22} M_{f2}^{(2)}}{\omega} F_2 & 0 \\ 0 & 0 & \frac{\beta_{23} M_{f2}^{(3)}}{\omega} F_3 \end{bmatrix} \quad (9)$$

where

$$F_i = \frac{(W_2^i - W_3^i) - (W_2^i + W_3^i) e^{2j\beta_{2i}(h_2 - h_1)}}{(W_2^i - W_3^i) - (W_2^i + W_3^i) e^{2j\beta_{2i}(h_2 - h_1)}}$$

and $j\beta_{1i} M_{f1}^{(i)} = W_1^i$, $j\beta_{2i} M_{f2}^{(i)} = W_2^i$, $\beta_c M_l^{(i)} = W_3^i$

From (9) and (4), sensor parameters can be evaluated for the 4-layer structure. It is noted that the sensitivity of the chemically sensitive layer depends on the degree of wave guidance provided by the first layer.

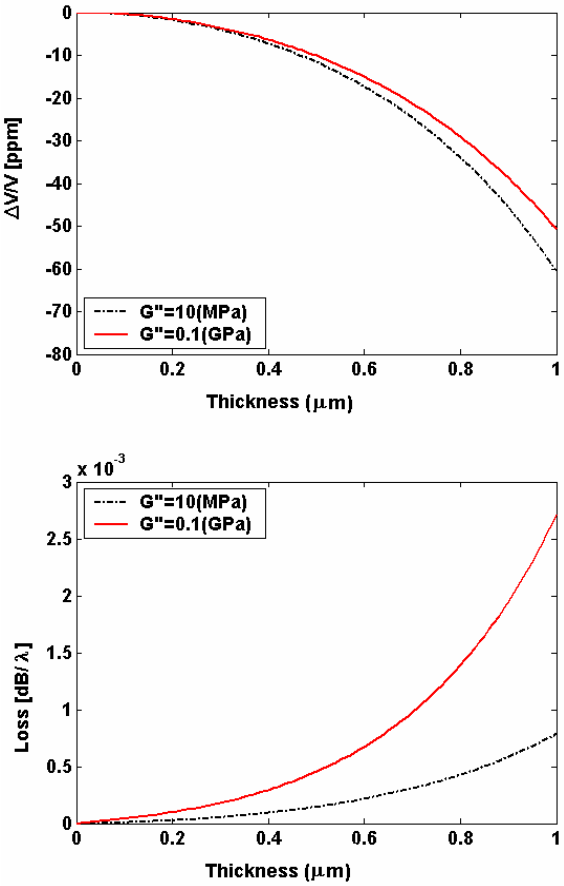

Fig. 2. Simulation results of velocity shift and loss change of the guided SH- SAW for the 3-layer sensor structure as a function of film thickness with G" as a parameter. In this simulation, G' = 1GPa

However, a complete analysis and determination of the sensitivity of this structure will require analyzing the function F_i. This will result in finding a range of thicknesses for the guidance layer (layer 1), necessary to optimize the device response. Preliminary theoretical analysis indicates that the 3-layer model is the more sensitive geometry. This is because the single layer is acting as both the guiding layer and the chemically sensitive layer. Therefore, any perturbation of that layer directly affects the wave guidance, hence the sensitivity.

Figures 2 and 3 show simulated results, for the 3-layer structure, of the velocity shift and loss change of the guided SH-SAW as a function of film thickness with G' or G" as a parameter. In both figures, it is clearly shown that the velocity and loss changes increase with increasing film thickness, which means the mass loading affects the sensor response. For a specific film thickness, it is noted that the velocity change and loss change both increase with decreasing G" in Fig.2. In Fig. 3, it is noted that the velocity change decreases with increasing G' and the loss change decreases with increasing G'. Both figures also show that the film viscoelastic properties definitely affect the sensor response, with such effect known as viscoelastic loading.

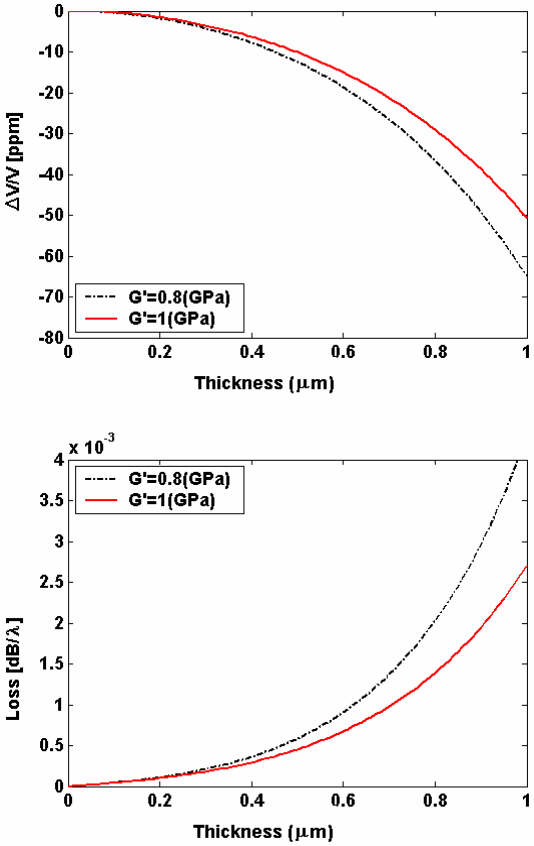

Fig. 3. Simulation results of velocity shift and loss change of guided SH-SAW for the 3-layer sensor structure as a function of film thickness with G' as a parameter. In this simulation, G" =0.1GPa

To simulate the mass loading effect in liquid-phase sensing, a polymer with thickness of 0.8 μm is assumed on the device. By slightly changing the density of the polymer

from 1.0 kg/m^2 to 1.2 kg/m^2, the velocity shift versus the area density ρh is calculated and shown in Fig. 4.

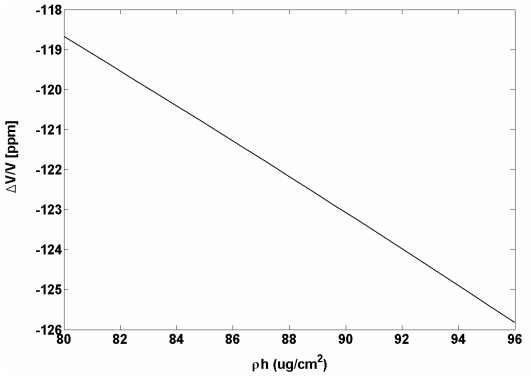

Fig. 4. Velocity shift as a function of mass loading

III. EXPERIMENTAL

The guided SH-SAW device used in this work is on the 36° YX-$LiTaO_3$ substrate with a polymer coating as the waveguide layer. The device is designed and fabricated with 100/800 nm thick Cr/Au interdigital transducers (IDTs) having a periodicity of 40μm. This corresponds to an operating frequency of approximately 103 MHz for the uncoated devices. A dual delay line configuration is used and consists of a reference line coated with polymethyl methacrylate (PMMA) which acts as a guiding layer only, and a sensing line coated with poly(isobutylene) (PIB), polyepichlorhydrin (PECH) or poly(ethyl acrylate) (PEA) which acts as both a guiding layer and a chemically sensitive layer. All polymers are used as purchased from Aldrich (Milwaukee, WI). The PMMA waveguiding layer is deposited on the device surface (over the IDTs and the delay path) by spin-coating solutions of 10, 15 or 20% w/v PMMA in 2-ethoxyethyl acetate, and then cured at 180°C for two hours. The PIB layer is deposited using 2.25~2.90% w/v in chloroform, PECH using 3~4% w/v in chloroform and PEA using 50~67% of commercially supplied PEA solution in toluene. The sensing coating's adhesion and stability are improved by exposing the device to the ambient air, or by heating the coated devices for 15 min at 40°C or 60°C. Film thicknesses of 0.5μm, 0.8μm and 1.0μm are obtained by using different solution concentrations and/or spin coating speeds. The thickness of PMMA films is determined using profilometry. For other polymer materials which are too soft for accurate characterization via profilometry, thicknesses are calibrated by using an identical coating methodology to deposit a film on a thickness shear mode (TSM) resonator. The Sauerbrey equation is used to determine film thicknesses from the TSM response. Care is taken to keep the thicknesses in the range (≤ 1 μm) where the Sauerbrey equation approximation is still valid.

A schematic diagram of the measurement system is shown in Fig. 5. The measurement system is composed of a network analyzer (Agilent 8753ES), switch/control unit (Agilent 3499A), guided SH-SAW device, PC-based HP VEE software for collecting data (loss, phase and frequency) and the auxiliary cables. A specially designed flow-through cell is used to expose each guided SH-SAW dual delay line to the chemical liquid-phase environment.

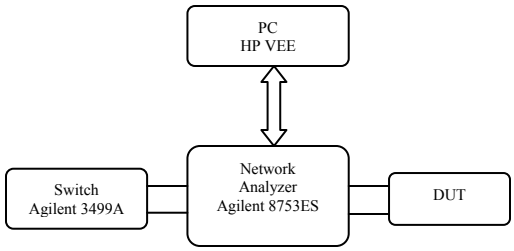

Fig. 5. Schematic diagram of the measurement system

The network analyzer is used for the initial device characterization, and for the sensing experiment together with a switch/control unit. The whole system includes the measurement system, the sensing system and the liquid sample delivery system. The sensing system consists of the guided SH-SAW devices, the mounting elements and a cell made from brass and lexan. The liquid sample delivery system consists of a pump, working solution vials, a waste tank and the connecting tubes. The working sample (1-60 ppm) is prepared by diluting the organic compounds in deionized (DI) water. A typical run is started by pumping DI water through the cell at a selected rate, then exposing the device to the analyte solutions. The selected low flow rate of 0.30 mL/min is used to minimize the hydrodynamic coupling between flowing liquid and the crystal surface, the pressure and pulsating flow effects on the sensor surface, which may add to the sensor noise. Prior to making measurements for a given analyte, the device coatings are conditioned by exposure to 50 ppm aqueous solutions of the analyte for 10 minutes in order to improve the stability of the device response. After conditioning, the device is alternately exposed for 10-minute periods to the DI water and the analyte solution. Here the DI water is used to make the response return to the baseline, demonstrating reversibility. The tested analytes include toluene, ethylbenzene and xylene in the low concentration (1 ppm to 60 ppm). Stability and sensitivity are investigated by varying the coating thickness 0.5 μm, 0.8 μm and 1.0 μm, or varying the curing temperature (room temperature, 40°C and 60°C) for different sensitive coatings (PIB, PECH and PEA).

IV. RESULTS AND DISCUSSION

Fig. 6 shows a typical response of a guided SH-SAW sensor device to varying concentrations of xylene (10-60 ppm) in DI water. On that device, the sensing line is coated with 0.8-μm-thick PIB cured at 40°C for 15 min while the same thickness of PMMA, cured at 180°C for 2h is used for the reference line. The result shows that for direct detection of 10 to 60 ppm of xylene in water, the sensor exhibits

excellent reversibility when the chemical analyte is removed. As indicated in the procedures, this is done by subjecting the device to DI water. In Fig.6, response time of 10 min is observed. However, the observed time in Fig.6 doesn't represent the sensor response time due to the use of the flow mixing system. A typical response time of the sensor is observed to be less than 30 seconds as chemical analyte is directly placed in contact with the device.

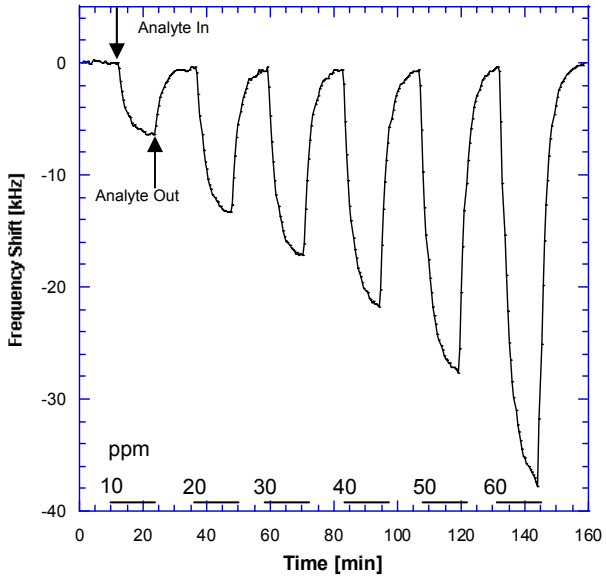

Fig.6. Detection of 10 to 60 ppm of xylene using a guided SH-SAW device with 0.8µm thick PIB on the sensing line and 0.8µm thick PMMA on the reference line. The PIB layer is uncured.

The observed frequency shift is reversible and linear with the analyte concentration. The observed slight deviation from linearity can be explained by fluctuations in the solution concentration due to the volatile nature of the analytes.

It is noted that Fig. 6 is not sufficient to determine the major contribution to the sensor response. These contributions can be due to mass loading and changes in viscoelastic properties of the polymer. Further insight into the various contributions to the sensor response can be obtained by simultaneously measuring the device loss as a function of analyte concentration. Figure 7 shows insertion loss in the xylene detection using the guided SH-SAW device with 0.8µm thick PIB on the sensing line and 0.8µm PMMA on the reference line. Clearly, the observed loss can be explained by changes in the viscoelastic properties of the load, i.e. chemically sensitive layer. As a result, both Fig.6 and Fig.7 clearly indicate that the two contributions to the sensor response are from the added analyte mass and subsequent changes in viscoelastic properties. However, the above is still not sufficient to determine the dominant contribution, assumed from past work to be from mass loading. Theoretical simulations (Figs. 2-4) and/or experimental determination of changes in viscoelasticity would provide that answer, which will allow for optimization of the sensor response. This is in part why the theoretical analysis and simulation are performed.

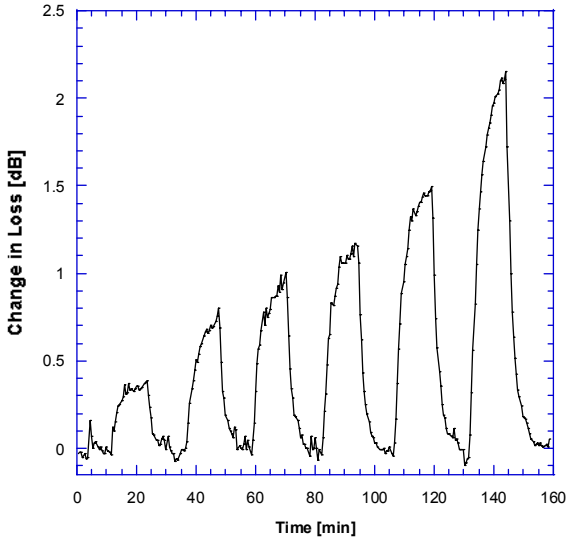

Fig. 7. Change in loss in the detection of 10 to 60 ppm xylene using the guided SH-SAW device with 0.8µm thick PIB on the sensing line and 0.8µm PMMA on the reference line

Thickness Effect: Fig. 8 shows the frequency shift (sensitivity) of the $LiTaO_3$ guided SH-SAW sensor device in the xylene detection with different coating thicknesses The reference line is coated with 0.5-, 0.8- or 1.0- µm -thick PMMA cured at 180°C for 2h while the chemical sensing line is coated with the same thickness of PIB, cured at 40°C for 15 min. It is seen that increasing the polymer thickness increases the sensitivity. In part, this is due to increased mass-loading in the thicker films. However, it is also expected that contributions from change in viscoelasticity will increase, especially the loss contribution. This is because the increase analyte concentration in the coating results in increase expansion in the polymer volume. The polymer becomes softer as it expands because of the polymer chain segments separation and the intermolecular attraction reduction, resulting in a decrease of polymer viscoelasticity (or increase in the loss modulus). Moreover, it is noticed that the response time is also increased with increasing thickness of the polymer, as expected. Thus a compromise in thickness must be made, combining a good sensitivity and fast response time. Such a tradeoff between high sensitivity and fast response results in an optimum PIB thickness of 0.5~0.8 µm.

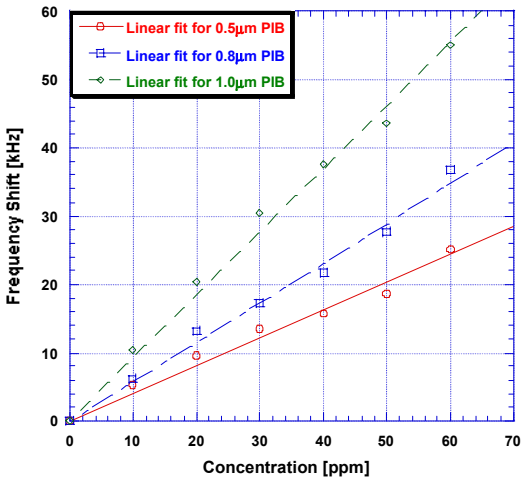

Fig.8. Comparison of sensitivity of PIB (0.5μm, 0.8μm and 1.0μm) – coated guided SH-SAW sensor platform in the detection of xylene in water (PIB is cured at 40°C for 15 min)

Polymer Curing Condition Effect: Fig. 9 shows the comparison of sensitivity of PIB-coated guided SH-SAW sensor platform with 0.5 μm-thick PIB cured at different temperature (uncured, 40°C, 60°C) for 15 min in the detection of toluene in water. It is shown that the sensitivity decreases when the curing temperature increases. Increasing the curing temperature, the residual solvent in the coating is evaporated further and the polymer molecule chain matrix is slightly shrunk and tightened making the analyte molecule entrapment difficult and needing a longer response time and recovery time. Hence, the smaller mass loading change will decrease the device frequency shift. Heating the coatings in this temperature range will result in the removal of residual solvent. This may lead to increased intermolecular interaction between the polymer chains, effectively decreasing the free volume in the coating (i.e. lowering the ability of the analyte to penetrate the coating) and also potentially changing the shear modulus. Another way of explaining this is that, at higher curing temperature, the polymer becomes more glassy, thus less prone to analyte adsorption. This can be also explained by the effect of mass loading change and polymer viscoelasticity decrease. In liquid environments, permeation of analytes into the polymer coating may also cause swelling and plasticization as in gas phase. The swelling effect results in a decrease in the overall modulus (decrease of the storage modulus and increase in the loss modulus) of the material regardless of whether the expanded volume occurs from analyte molecules or only free volume. When the polymer is cured at higher temperatures, the analyte may not produce the same degree of swelling and/or plasticization, resulting in the smaller decrease of the shear modulus (or smaller increase of the shear loss modulus) of the coating. This, in turn, produces smaller change in the acoustic wave velocity, hence frequency shifts of the device. At higher curing temperature, smaller device loss as a function of analyte concentration is also observed. However, the sensor stability also increases and sensor signal noise decreases when the coatings are cured at higher temperature. Again, the result is a tradeoff between high sensitivity and stability, with curing of the coating at 40°C providing a good compromise.

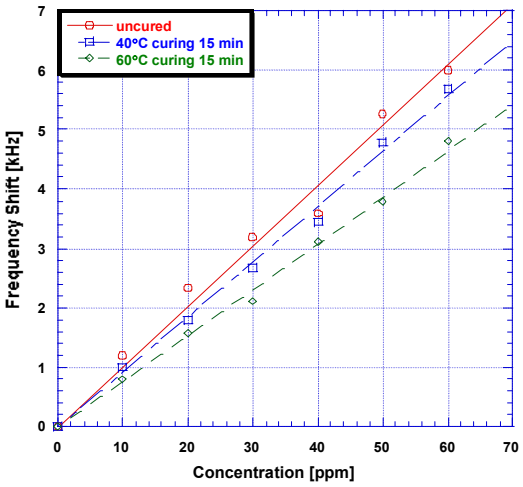

Fig.9. Comparison of sensitivity of PIB-coated Guided SH-SAW sensor platform with 0.5 μm thickness cured at different temperature (concurred, 40ºC, 60ºC) in the detection of Toluene in water

Partition Coefficients: The sorption process in liquid-phase sensing can be described by the partition coefficient, $K_{P\text{-}L}$, which is a thermodynamic parameter that characterizes the distribution of organic analytes between the polymer coating and the aqueous solution [11]. Calculation of $K_{P\text{-}L}$ can be used to predict the inherent selectivity of a sensor coating material in liquid environment and is given by

$$K_{P-L} = \frac{C_P}{C_L} = \frac{C_P / C_A}{C_L / C_A} = \frac{K_{P-A}}{K_{L-A}}$$

$$LogK_{P-L} = LogK_{P-A} - LogK_{L-A} \qquad \textbf{(10)}$$

C_P, C_A and C_L are the concentrations of analyte molecules in the polymer coating, air and liquid, respectively. $K_{P\text{-}A}$ and $K_{L\text{-}A}$ are the partition coefficients of polymer-air and liquid-air pairs. $K_{P\text{-}A}$ and $K_{L\text{-}A}$ can be calculated using a linear solvation energy relationship (LSER) [12], provided that the appropriate LSER parameters are available. $K_{P\text{-}L}$ is a good estimate of the relative response of a particular coating to a series of analyte solutions or of a series of polymer coatings to a given analyte. $K_{L\text{-}A}$ is thus directly related to mass loading.

In addition to the mass-loading contribution to a sensor response [13], the observed frequency shift, Δf_v, also has a contribution from the swelling-induced modulus change [14,15]. A model which includes both contributions has been developed for gas sensing applications [16,17], and is given by

$$\Delta f_v = \left(\frac{\Delta f_s C_A K}{\rho_s}\right) + f_A \left(\frac{C_A K}{\rho_A}\right)\left(\frac{\Delta f_s A_{SAW}}{\alpha}\right) \qquad (11)$$

In (11), the first term represents the effect of mass loading and the second term represents the swelling-induced modulus change. In this equation, Δf_s represents the

frequency shift due to the amount of sorbent phase; ρ_s is the density of the sorbent phase; ρ_A is the density of the vapor as a liquid; A_{SAW} represents the kilohertz change in frequency due to a 1°C change in temperature per kilohertz of coating on the device surface; α is the coefficient of thermal expansion of the polymer, i.e., the fractional volume increase per degree; and f_A is the fractional free volume of the diluent (vapor) as a liquid. The parameters in (11) consist of those that are vapor-dependent, f_A and ρ_A, and those that are strictly polymer-dependent, ρ_s, A_{SAW} and α. The SAW response to vapor sorption is therefore affected by the sum of the mass loading effect and the modulus effect, which is modeled in terms of free volume changes due to thermal expansion.

By analogy, a similar equation for the guided SH-SAW sensor can be derived for liquid-phase detection where ρ_L is the density of the liquid analyte and $A_{SH\text{-}SAW}$ represents the kilohertz change in frequency due to a 1°C change in temperature per kilohertz of coating on the guided SH-SAW device surface. A preliminary expression for the total frequency shift in liquid, based on eq. 10, is given by

$$\Delta f_v = \left(\frac{\Delta f_s C_L K_{P-L}}{\rho_s}\right) + f_L\left(\frac{C_L K_{P-L}}{\rho_L}\right)\left(\frac{\Delta f_s A_{SH-SAW}}{\alpha}\right) \qquad \textbf{(12)}$$

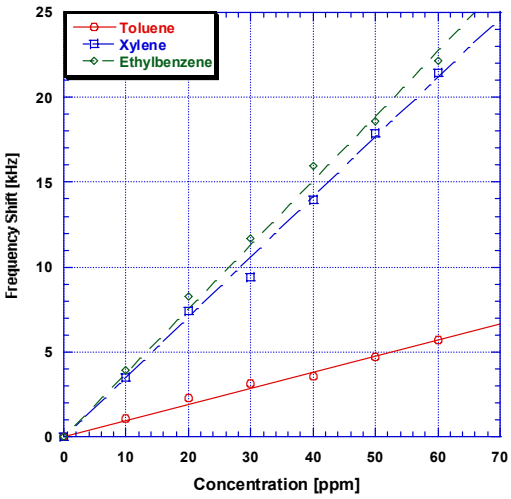

Fig.10. Comparison of selectivity of PIB-coated (with 0.5µm thickness, uncured) guided SH-SAW sensor platform in the detection of toluene, xylene and ethylbenzene in water.

Three organic compounds (ethylbenzene, toluene, xylene) in water are detected using a PIB-coated (0.5µm, uncured) guided SH-SAW sensor platform. Fig. 10 shows the response of PIB-coated device to toluene, xylene and ethylbenzene. And it is noticed that PIB is least sensitive to toluene and most sensitive to ethylbenzene. The device responses and partition coefficients calculated using literature data [11,12] are normalized with respect to the toluene data and are compared in Fig. 11. The observed frequency shifts are in agreement with the predicted trend from the partition coefficients. The small discrepancies may be due to the fact that partition coefficients do not include the modulus effect discussed above. Further work is necessary to determine whether (12) can be used to more accurately model the sensor response. However, partition coefficient data can still be used for an approximate classification and selection of the coatings.

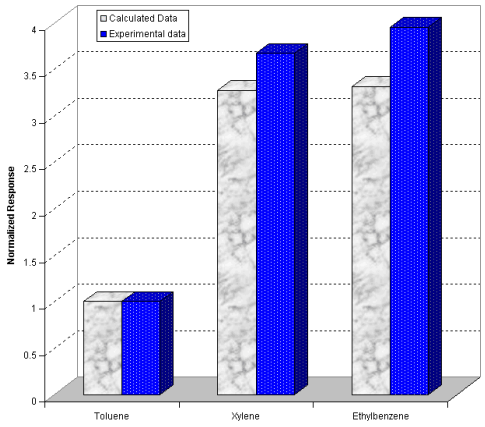

Fig.11. Comparison of calculated normalized partition coefficient and normalized experimental data

Three different polymer coatings, PIB, PECH and PEA, are investigated in the present study as chemically sensitive layers on the guided SH-SAW device. Devices coated with 0.8 µm thick of each layer cured at 40ºC for 15 minutes are tested in the detection of xylene in water. Results comparing the sensitivity of the polymers to xylene are shown in Fig. 12, with PEA showing the highest sensitivity.

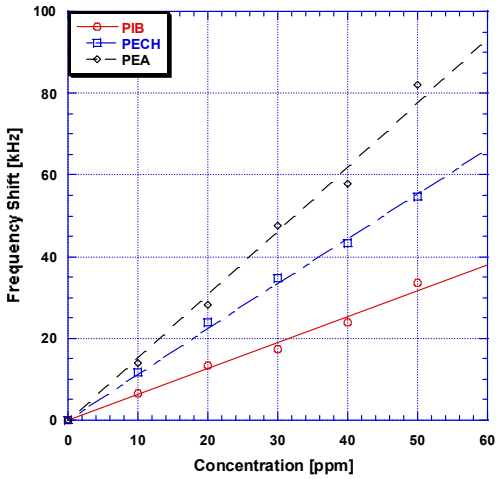

Fig.12. Comparison of sensitivity of Polymer (PIB, PECH, PEA)-coated guided SH-SAW sensor platform with 0.8µm thickness cured at 40ºC for 15 minutes in the detection of xylene in water

Detection Limit: The detection limit is defined here as a measured signal that is no smaller than three times peak-to-peak or three times the root-mean-square noise level. The detection limit of a sensor depends on two factors, the sensor sensitivity and the signal stability due to the noise and drifts, etc. The contributions to device sensitivity due to mass density and coating viscoelastic property changes can be determined, and the devices optimized, by investigating the thickness effect, curing condition effect, etc. Signal

noise, on the other hand, depends on the device frequency of operation, coating stability in water, but also on the flow system and measurement system/circuit. A detection limit of 100 ppb (3×peak-to-peak noise) or 25 ppb (3× root-mean-square noise) can be estimated from the present measurements for ethylbenzene, 130 ppb or 30 ppb for xylene, and 300 ppb or 75 ppb for toluene. Fig. 13 shows the detection of 1 ppm toluene, xylene and ethylbenzene detection using 0.8-μm-thick uncured PECH-coated SH-SAW device. Clearly, a detection limit of the order of 10 ppb or less can be achieved with the present sensor platform for some analytes in aqueous environments.

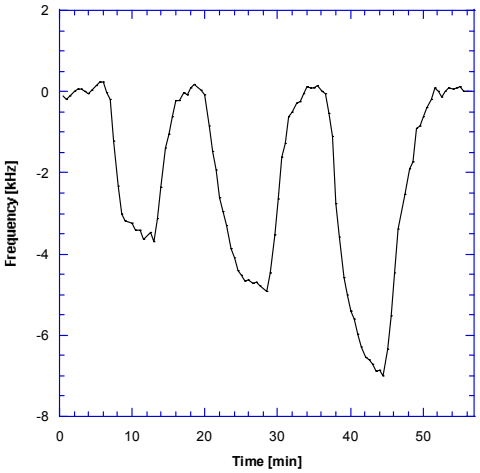

Fig. 13. Comparison of sensitivity and partial selectivity of polymer PECH with 0.8μm thickness uncured device in the detection of 1 ppm Toluene, Xylene and Ethylbenzene

V. Conclusion

The guided SH-SAW device on 36° YX-$LiTaO_3$ substrate has been proven to be one of the most sensitive acoustic wave liquid-phase detectors. A number of factors can affect the responses of polymer-coated SH-SAW sensors in liquid environments, such as mass density, film thickness, liquid properties, and film shear modulus. As indicated by both theoretical analysis and experiments, the primary contributions to the sensor response are from the changes in mass loading and polymer viscoelasticity, both the result of analyte sorption in the coating. However, effective implementation of the sensors requires investigating various chemically sensitive layers, coating thickness and curing methodologies for higher sensitivity and stability. Uncured chemically sensitive coating (viscoelastic) show higher sensitivity to analyte sorption from water, but low temperature curing (T=30~60°C) of the chemically sensitive layer is necessary for some degree of stability in aqueous environments. In general, a compromise has to be made to find the optimal coating thickness in terms of the sensitivity, stability, response time and partial selectivity. The detection limits obtained from present experiments is of the order of 10 ppb for the analytes toluene, ethylbenzene, and xylene using an appropriately selected coating.

Partition coefficient calculations for coating-analyte pairs further proved that the liquid-phase sensor response is affected by mass loading and the decrease in the shear modulus of the polymer coating. Good agreement is obtained between calculated partition coefficients and experiments results. As a result, despite the complex detection process (i.e. competition between water molecules and analytes) in liquid-phase, partition coefficient calculation should always be the first step in the selection of the polymer coating, as in gas-phase.

Polymer-Guided-SH-SAW sensor platforms thus can be used for the direct, rapid and reproducible detection of chemical contaminants in liquids. Based on the present data, sensor arrays can be built, which utilize both the device loss data and frequency shift data for pattern recognition.

Acknowledgment

This work is partially supported by NSF grant Nos: ECS-9876366, ECS-0110381 and CHE-0074962.

References

[1] D.S. Ballantine, R.W. White, S.J. Martin, A.J. Ricco, G.C. Frye, E.T. Zeller and H. Wohltjen, "*Acoustic wave sensors: theory, design, and physical-chemical applications*," Academic Press, 1996

[2] F. Josse, F. Bender and R. W. Cernosek, "Guided shear horizontal surface acoustic wave sensors for chemical and biochemical detection in liquid," *Anal. Chem.* 2001, 73, pp. 5937-5944

[3] G. L. Harding, J. Du, P. R. Dencher, D. Barnett and E. Howe, "Love wave acoustic immunosensor operating in liquid," *Sensors and Actuators,* A61, 1997, pp. 279-286

[4] F. Bender, R. W. Cernosek and F. Josse, "Love-wave biosensors using cross-linked polymer wave guides on $LiTaO_3$ substrates," *Electronics Letter*, 36 (19), 2000, pp. 1672-1673

[5] R. Patel, R. Zhou, K. Zinszer and F. Josse, "Real-time of organic compounds in liquid environments using polymer-coated thickness shear mode quartz resonators," *Anal. Chem*. 2000, 72, pp. 4888-4898

[6] C. McMullan, H. Mehta, E. Gizeli and C.R. Lowe, "Modelling of the mass sensitivity of the love wave device in the presence of a viscous liquid", *J. Phys. D.: Appl. Phys.* 33, (2000) pp. 3053-3059

[7] J. Kondoh and S. Shiokawa, "A liquid sensor based on a shear horizontal SAW device," *Electronics and Communications in Japan*, Part 2, 76 (2), 1993, pp. 69-81

[8] S. J. Martin and G. C. Frye, "Dynamics and response of polymer-coated surface acoustic wave devices: effect of viscoelastic properties and film resonance," *Anal. Chem,* 1994, 66, pp. 2201-2219

[9] J. Kondoh, K. Saito, S. Shiokawa and H. Suzuki, "Simultaneous measurements of liquid properties using multichannel shear horizontal surface acoustic wave microsensor", *Jpn. J. Appl. Phys.* Vol. 35 (1996), pp. 3093-3096

[10] J. Kondoh, S. Shiokawa, M. Rapp and S. Stier, "Simulation of viscoelastic effects of polymer coatings on surface acoustic wave gas sensor under consideration of film thickness," *Jpa. J. Appl. Phys.* Vol. 37 (1998), PP. 2842-2848

[11] R. A. McGill, "Choosing polymer coatings for gas and liquid chemical microsensors," *SPE ANTEC Indianapolis Proceedings,* 1996, pp.2080-2084

[12] R. A. McGill, M. H. Abraham and J. W. Grate, "Choosing polymer coatings for chemical sensors," *Chemtech* 1994, 24 (9), pp. 27-37

[13] Z. Liron, N. Kaushansky, G. Frishman, D. Kaplan and J. Greenblatt, "The polymer-coated SAW sensor as a gravimetric sensor," *Anal. Chem.* 1997, 69, pp. 2848-2854

[14] J. W. Grate and S. N. Kaganove, "Comparisons of polymer/gas partition coefficients calculated from responses of thickness shear

mode and surface acoustic wave vapor sensors," *Anal. Chem*. 1998, 70, pp. 199-203

[15] J. W. Grate, S. J. Patrash and M. H. Abraham, "Method for estimating polymer-coated acoustic wave vapor sensor responses," *Anal. Chem.* 1995, 67, pp. 2162-2169

[16] J.W. Grate and E. T. Zellers, "The fractional free volume of the sorbed vapor in modeling the viscorlastic contribution to polymer-coated surface acoustic wave vapor sensor responses," *Anal. Chem.* 2000, 72, pp 2861-2868

[17] J. W. Grate, M. klusty, R.A. McGill, M.H. Abraham, G. Whiting and J. Aandonian-Haftvan, "The predominant role of swelling-induced modulus changes of the sorbent phase in determining the responses of polymer-coated surface acoustic wave vapor sensors," *Anal. Chem.* 1992, 64, pp.610-624